Published in the Journal of Magnetism and Magnetic Materials, 564, 170115 (2022)

Ultra-low anisotropy magnetoelectric sensor in ferrite/piezoelectric toroidal composites

Bingfeng Ge¹, Jitao Zhang^{1†}, Qingfang Zhang¹, D. A. Filippov², Jie Wu¹, Jiagui Tao³, Jing Chen³, Liying Jiang¹, Lingzhi Cao¹, and Gopalan Srinivasan⁴

¹College of Electrical and Information Engineering, Zhengzhou University of Light Industry, Zhengzhou 450002, China

An ultra-low anisotropy magnetoelectric (ME) magnetic field sensor consisting of strictly concentric toroidal nickel-zinc ferrite/piezoelectric composite with toroidal solenoid was developed, and its sensitivity and resolution under different angles of planar AC/DC magnetic field were systemically characterized. The experimental results demonstrate that the induced voltage output strength was constant along the angles between the ME magnetic sensor and the planar DC/AC magnetic field due to toroidal structure had ultra-low shape-induced anisotropy. Consequently, for the DC case its sensitivity and resolution could reach about 15 mV/Oe and $2 \times 10^{-7} \text{T}$ under a low excitation of f=111.42kHz circumferential AC magnetic field, respectively. Correspondingly, for the AC case its sensitivity and resolution could reach about 56.9 mV/Oe and $7 \times 10^{-9} \text{T}$ under a 2.25Oe circumferential DC bias magnetic field. These findings provided more flexibility of the device design for weak magnetic field detection.

I. INTRODUCTION

In recent years, the attention for magnetic sensors is continuously increasing due to enormous economic-effective, and they have extensive applications in the vehicle navigation[1], the detection of bio-magnetic[2], non-destructive testing[3], medical sensors[4], and even the electroencephalogram detection, *etc*[5, 6]. Currently, various technologies have been used for magnetic sensing, such as search coil[7], fluxgate[8], hall-effect[9], superconducting quantum interference device[10], magnetoelectric effect[11], optical pump magnetometer[12], magnetoresistance[13], *etc*. Among these

† Corresponding author: Tel. /Fax: +86 371 86601601. E-mail address: zhangjitao@zzuli.edu.cn (J. T. Zhang)

1

²Institute of Electronic and Information Systems, Novgorod State University, Veliky Novgorod 173003, Russia

³State Grid of Jiangsu Electric Power Co., Ltd. Nanjing 210024, China

⁴Physics Department, Oakland University, Rochester, Michigan 48309, USA

technologies, the ME magnetic sensors are composed of magnetostrictive/piezoelectric composites drawn much research attention as they are cost-effective, miniaturization, highly sensitive, and simple operation, and the applications of ME magnetic sensors have been enormously reported. For instance, Dong et al., demonstrated that the output voltage of a long-type ME laminate magnetic sensor consisting of Terfenol-D and PZT with an exceptionally linear response to an AC magnetic field H_{AC} was found over the range of $10^{-11} < H_{AC} < 10^{-3} T[14]$. Subsequently, Dong et al. reported the long-type ME laminate magnetic sensor consisting of Terfenol-D and PZT, which exhibit a DC magnetic field sensitivity of 10⁻⁸T under a constant drive of H_{AC}=10e[15]. Recently, a ME magnetic sensor based on Metglas/quartz composites was presented by Sun et al, with an extremely high AC magnetic field sensitivity of 44pT±1.41pT for low frequency(1-100Hz)[16]. Yang et al. demonstrated a long-type arc shaped Metglas/polyvinylidene fluoride (PVDF)/Ni ME laminate with a self-biased effect, which reveal an AC magnetic field sensitivity of 10⁻⁹T under a wide detection range (1-25 kHz)[17]. Chen et al. reported a wireless millimetric magnetoelectric implant consisting of Metglas/PZT for the endovascular stimulation of peripheral nerves, which size is only 3×2.15×14.8mm³ and can achieve minimally invasive implants without open surgery[18]. Focused efforts in previous reports were devoted to detecting planar DC/AC magnetic field by using long-type ME magnetic sensor consisting of magnetostrictive/piezoelectric composites, which has high ME coefficient and high sensitivity. However, such structure meanwhile has significant shape-induced anisotropy, which will seriously affect ME coupling coefficient when the angle between the direction of magnetization of ME magnetic sensor and the planar DC/AC magnetic field are not parallel, proceed to cause enormous deviation and affect the stability of ME magnetic sensors[19, 20]. For example, Zhang et al. revealed long-type magnetostrictive materials with specific crystal orientation is highly anisotropic, which the magnetostriction coefficient decreases when changing magnetization direction due to the demagnetization effect[21]. Cui et al. revealed an effective of size effect and demagnetization effect on the ME coupling coefficient in piezoelectric/piezomagnetic laminates, which predicted that as sizes of ME laminates decrease from 100mm to 10⁻¹ ³mm, ME coefficient will dramatically decrease from 5 V/cm Oe to 0.08V/cm Oe correspondingly[22]. Zhang et al. demonstrated that the effect of DC magnetic field direction on the ME voltage coefficient (MEVC) measured for ME composites consisting of NZFO/PMN-PT, which observed a maximum MEVC of 114.4V/cm Oe at θ =0° and the MEVC decreased to 58.2V/cm Oe when H_{DC} direction at θ =90° under H_{DC}=23Oe[23]. In various practical applications like position detection, vehicle information and communication system, precision machining, etc.[24, 25], it is inevitable that the magnetic field direction cannot be strictly parallel to the direction of magnetization of magnetic sensor, which cause a slight deviation from the real data, resulting in poor precision. Particularly, in high-precision applications, the deviation could seriously affect the stability of devices, so magnetic field sensors with low anisotropy have great potentials in practical applications.

In this study, a toroidal ME magnetic sensor in composite of strictly concentric ferrites/piezoelectric ring with toroidal solenoid wound around it was fabricated and

developed. Compared with the previously reported ME magnetic sensors of long-type laminate configurations, the toroidal ME magnetic sensor has ultra-low shape-induced anisotropy and strong ME couplings, which output is almost immune from the angle between the ME magnetic sensor and the magnetic field. These favorable characteristics including low shape-induced anisotropy and strong ME couplings offer unique possibilities for use of magnetic sensors. In addition, the measurements of sensitivity and resolution for the presented toroidal ME magnetic sensor were implemented.

II. SAMPLE FABRICATION AND EXPERIMENT

Polycrystalline nickel-zinc ferrite cylinder with composition of Ni_{0.8}Zn_{0.2}Sm_{0.02}Fe_{1.98}O₄ (abbreviated as NZSFO) was synthesized by conventional solid-state method, commercially purchased powders of NiO, ZnO, Sm₂O₃ and Fe₂O₃ with purity of 99.9% were fully mixed in stoichiometric ratio, ball-milled, pre-sintered at 800°C, followed by ball milling, pressed pellets and then final sintered at 1275 °C with heating/cooling rate of 2°C/min in a muffle furnace[26]. Sintered ferrite cylinder was sliced into thin discs with 14mm in diameter and 1mm in thickness by a lowfrequency diamond saw. NZSFO was selected as magnetostrictive phase due to its soft magnetic properties (easy magnetization and demagnetization), and light samarium doping was intended to improve the dynamic magneto-mechanical conversion while decrease the hysteresis losses[27, 28]. Commercially purchased hard piezoelectric ceramic of PbaS-4 disc with similar dimensions were selected due to its relatively lower hysteresis losses (quality factor approximates 2200). Tri-layer strict concentric sample of NZSFO/ PbaS-4/ NZSFO was fabricated by bonding ferrite and piezoelectric slab together with epoxy adhesive (Vishay M-Bond 600 kit) and was cured at 120°C for 2h, followed by a round hole drilling with dimeter of 8mm. Finally, the sample was packaged in a non-magnetic fixture shell while the enameled copper was tightly wound with diameter of 0.15mm to provide a toroidal solenoid of ~90 turns per arc. The schematic diagram and photograph of the proposed toroidal magnetic sensor was illustrated in Fig. 1(a), and the details about the toroidal sample package can be found in our previous literature. The AC/DC magnetic field was produced by a 200-turn copper solenoid with a current source (Keithley Model 6221). Typical parameters such as sensitivity and resolution of presented toroidal ME magnetic sensor were measured using a lock-in amplifier (Zurich Model MFLI-500kHz). The working principle of the toroidal ME magnetic sensor for DC magnetic field detection mode was shown in Fig.1(b). A weak constant circumferential AC magnetic field, produced from toroidal solenoid, was used to excite the sample into vibration along its circumferential axis to generate voltage, and the induced voltage of toroidal ME composites will change with the variation of the superimposed DC magnetic field. Correspondingly, the working principle of toroidal ME magnetic sensor for AC magnetic field detection mode was shown in Fig. 1 (c), an optimum circumferential DC bias magnetic field was applied to the sample, which enables the improvement the MEVC of ME composites as well as eventual the sensitivity of presented sensor. Then, a lock-in amplifier was also employed to capture the induced ME voltage.

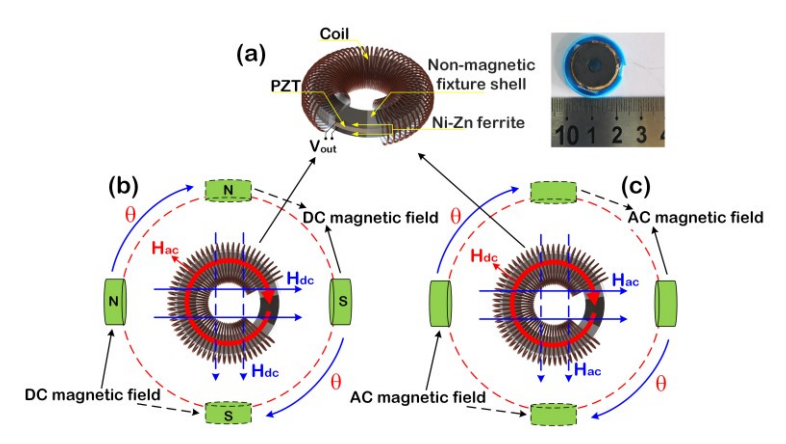


Fig. 1. (a) Schematic diagram and photograph of presented toroidal ME magnetic sensor. (b) The working principle of toroidal ME magnetic sensor for DC magnetic field detection mode. (c) The working principle of toroidal ME magnetic sensor AC magnetic field detection mode.

III. RESULTS AND DISCUSSIONS

Magnetostrictive layer as the actuating layer of ME composite material will produce a strain to realize the conversion of "magneto-mechanical" under an action of alternating magnetic field[29, 30]. Accordingly, the magnetic properties of magnetostrictive layer are significant to evaluate the performance of ME coefficient of ME composite material[31, 32]. The magnetic field distribution inside the toroidal ME composite with dimensions of inner diameter 8mm outer diameter 14mm and the longtype ME composite with dimensions of 14mm×4mm×1mm were analyzed by the simulations under the magnitudes of H_{DC} fixed at 50Oe, and simultaneously magnetic field rotates 45° each time within the range of 0°-135°. As illustrated in Fig. 2(a)-(d), the magnetic flux density distributions of the toroidal magnetostrictive material in x-y plane can be clearly observed. The inhomogeneous distribution of the magnetic flux density due to edge effects, and the maximum modulus occurring at the region where the toroidal sample is tangent to the magnetic flux density direction [33]. And as θ is increased from 0° to 135° with increment of 45°, the magnetic flux density distribution always remains in this condition, thus demonstrating that the direction of magnetic field will not affect the distribution of magnetic flux density in toroidal magnetostrictive material. Fig. 2(e)-(h) shown the magnetic flux density distributions of the long-type magnetostrictive material in x-y plane of Cartesian coordinate, which the inhomogeneous distribution of the magnetic flux density can also be clearly observed due to edge effects and demagnetization effects. Nevertheless, different with toroidal sample from the toroidal sample that the intensity of flux density distribution varies with the direction of the magnetic field due to the high shape-induced anisotropy of long-type sample, and the maximum magnetic flux density decreases from 4×10⁻²T to 1.2×10⁻²T when magnetic field rotates from 0° to 90°. From the simulation results obtained above, long-type magnetostrictive material have a significant attenuation in magnetization with θ rotations, by contrast, the toroidal magnetostrictive material will not have such a situation. Furthermore, we infer from the results that the variations in magnetization will directly affect the dynamic magneto-elastic couplings of long-type magnetostrictive material, and influence magnetoelectric voltage response of long-type ME composites. But the magnetoelectric voltage response of the toroidal ME

composites will not be affected by the direction of magnetic field. To demonstrate that, magnetoelectric voltage characterizations of long-type and toroidal ME composites will be implemented as follows.

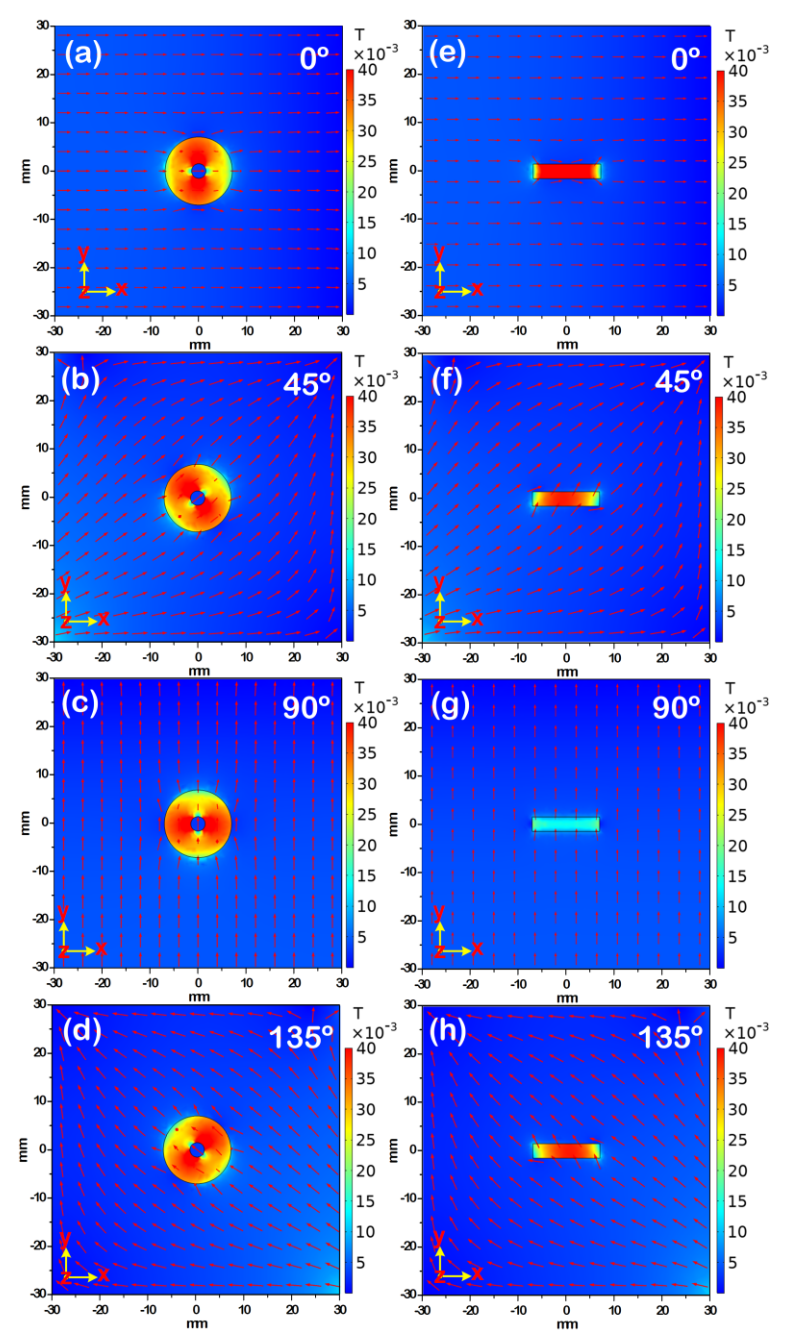


Fig. 2 Magnetic flux density distributions in *x-y* plane of toroidal NZFO sample for θ =(a)0°(b)45°(c)90°(d)135° and long-type NZFO sample for θ =(e)0°(f)45°(g)90°(h)135° at H_{DC}=50Oe

To further clarify the influences of θ on ME voltage output, toroidal and long-type composite materials for various θ were measured in the range of 0° and 360° . Fig. 3 (a) shown the ME voltage output of the toroidal ME magnetic sensor when the DC magnetic field with different directions and different intensities (1.00e, 1.10e and 1.20e, respectively) was applied in the plane of the sample. Clearly, the voltage output of toroidal ME magnetic sensor hardly changed with the change of planar DC magnetic

field angle, mainly due to the toroidal structure employed, which has lower shapeinduced anisotropy, near-zero demagnetization effect and high-frequency noise suppression relative to its counterparts. The inset of Fig. 3 (a) shown the direction of the DC magnetic fields in a top view. Fig. 3 (b) shown the ME voltage output of the toroidal ME magnetic sensor when the AC magnetic field with different directions and different intensities (10e, 1.10e and 1.20e, respectively) was applied in the plane of the sample. The voltage output of toroidal ME magnetic sensor hardly changed with the change of planar AC magnetic field angle, and inset of Fig. 3 (b) shown the direction of the AC magnetic fields in a top view. Fig. 3 (c) illustrated the ME voltage output of the long-type ME magnetic field sensor as a function of direction of magnetic field at $H_{DC} = 5$ Oe. Clearly, the voltage output of long-type ME magnetic sensor rapid decrease from 36.7mV to 8.2mV When the magnetic field angle is from 0° to 90°, which reduced by 77.65%, and then the induced voltage decreases and increases periodically every 90 degrees. It is found that a large dependence on θ of the ME voltage for long-type ME magnetic sensor, mainly due to the demagnetizing effect. The inset of Fig. 3 (c) shown the direction of the DC magnetic fields in a top view. As illustrated in Fig. 3 (d), the ME voltage output of the long-type ME magnetic sensor as a function of direction of magnetic field at a 52.2kHz 1Oe AC magnetic field. The result shows the voltage output of long-type ME magnetic sensor suddenly decrease from 28.8mV to 13.9mV When the magnetic field angle is from 0° to 90°, which reduced by 51.7%, and then the induced voltage decrease and increase periodically every 90 degrees. The inset of Fig. 3 (d) shown the direction of the DC magnetic fields in a top view. Compared with the long-type configurations schemes, toroidal configuration would not cause enormous deviation due to the angle between the sample and the magnetic field when measuring the planar magnetic field. Therefore, the toroidal ME magnetic sensor had better stability, which was beneficial for sensor.

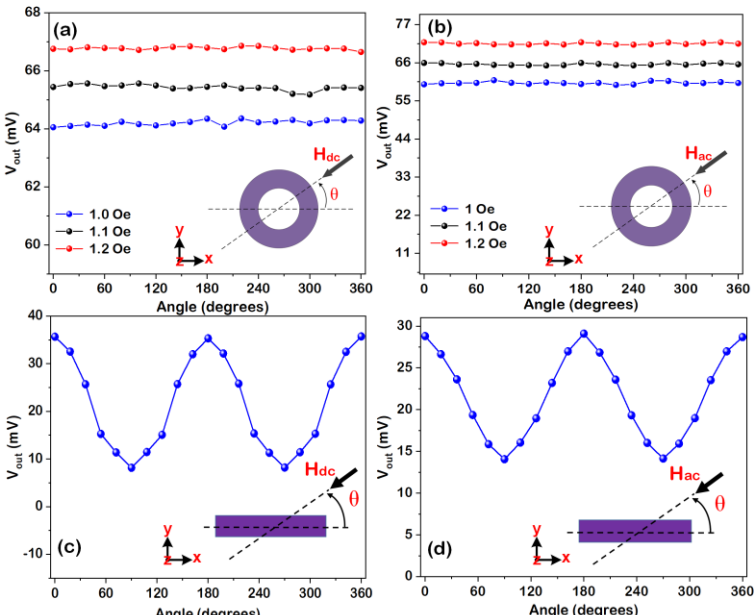


Fig. 3 (a) The effect of DC magnetic field angle on the ME output voltage measured for toroidal ME sensor. (b) The effect of AC magnetic field angle on the ME output voltage measured for toroidal ME sensor. (c) The effect of DC magnetic field angle on the ME output voltage measured for long-type ME sensor. (d) The effect of

In order improve the sensitivity of ME magnetic sensor as much as possible, one would expect stronger MEVC[34, 35]. As illustrated in Fig. 1(b) that a weak circumferential AC drive field is required for the toroidal ME magnetic sensor when detecting the DC magnetic field. And the maximum ME induction voltage output was usually obtained when the drive signal frequency was resonant with the ME composite material. Fig. 4(a) shown the MEVC for toroidal ME composites as a function of circumferential AC magnetic field frequency under condition that the planar DC magnetic field is zero, a giant sharp resonance peak with value of 31.09V/cm Oe is observed at the resonance frequency of 111.42 kHz, and the MEVC is nearly two orders of magnitude higher than non-resonant modes when toroidal ME composites works in the resonance state. Therefore, a 111.42kHz circumferential AC magnetic field should be provided for the toroidal ME magnetic field sensor when measuring the DC magnetic field. Then induced ME voltage output versus the circumferential bias magnetic field were measured at the resonant frequency of 111.42kHz. As illustrated in Fig. 1(c) that a circumferential DC excitation field is required for the toroidal ME magnetic sensor when detecting the AC magnetic field. The circumferential DC bias magnetic field can attenuate the demagnetization effects exerted by the planar AC magnetic on ME composite material, proceed to enhance the ME induction voltage output. Fig. 4(b) shows the variation of induced ME voltage coefficient under different circumferential bias DC magnetic field for toroidal ME composites sample when external planar AC magnetic field is 10e and f=111.42 kHz. Here, the induced MEVC shows strong dependence with circumferential bias DC magnetic field with the field varied from zero. The MEVC increases with an initial non-zero value of 0.387V/cm Oe, and then it increases rapidly to a maximum value of 0.659V/cm Oe at optimum bias of 2.25Oe then decreases sharply. Therefore, in order to obtain a higher sensitivity as much as possible when detecting planar AC magnetic field, it is necessary to apply a 2.25Oe circumferential bias magnetic field.

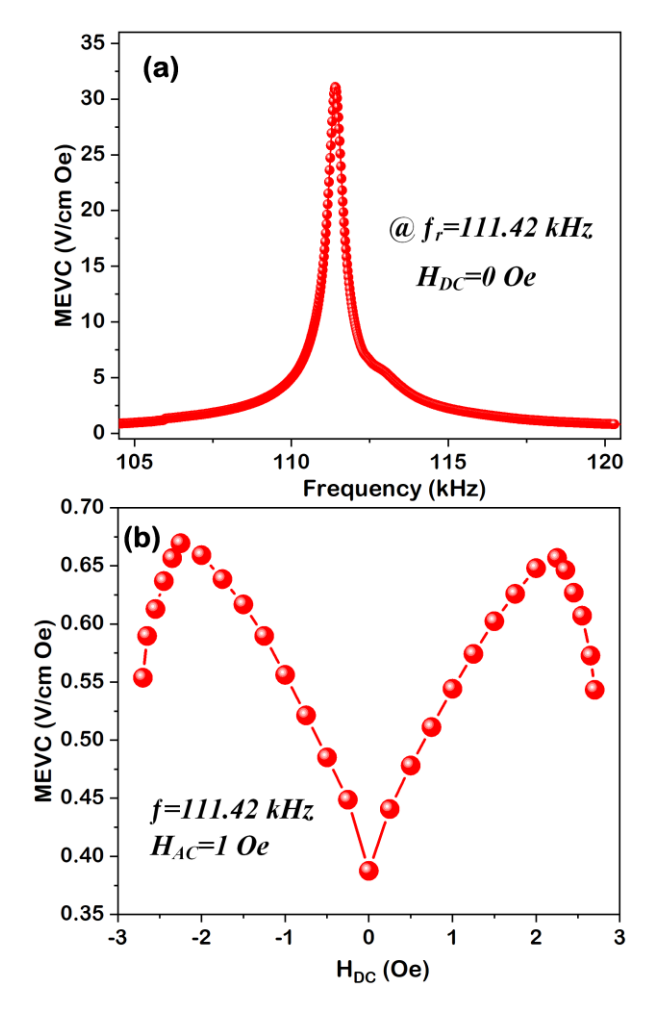


Fig. 4 (a) The ME voltage coefficient dependence of frequency in the range of 104 kHz-122 kHz without planar DC magnetic field. (b) Induced ME voltage as a function of circumferential DC magnetic field under a 10e of f=111.42 kHz planar AC magnetic field.

To evaluate the capabilities of DC magnetic field detection for toroidal ME magnetic sensor, the output sensitivity and resolution were measured under a 111.4 2kHz low circumferential AC excitation. The DC magnetic field sensitivity and resolution were characterized for toroidal ME magnetic sensors using an active method: a 400-turn toroidal solenoid was wrapped around the toroidal sensor that carried a tiny AC current provided by the lock-in amplifier to drive the ME sensors. The toroidal ME magnetic field sensor was fixed in the center of the Helmholtz coil, a current source (Keithley Model 6221) generated a DC current as an input to the Helmholtz coil, and the lock-in amplifier (Zurich Model MFLI-500kHz) was used to measure the output signals. Fig 5 (a) shown the sensitivity of the induced ME voltage responding to the variations of DC magnetic field strength, and the induced ME voltage exhibits an approximately linear relationship with the DC magnetic field strength over the range of approximately (0.20e-2.60e). The errors in the measurement of DC magnetic field sensitivity were caused by the self-characteristics of ME composite (such as the hysteresis, demagnetization effect). The measured sensitivities under a 111.42 kHz low circumferential AC excitation conditions were about 15mV/Oe. The inset of Fig 5 (a)

shown the induced ME voltages from the toroidal ME magnetic sensor in response to little changes in H_{DC} at driving frequency of a f=111.42kHz low circumferential AC excitation. The DC magnetic field generated by Helmholtz coil was $H_{DC}=2\times10^{-7}T$. The induced ME voltage output was about 55.44 mV under this low DC magnetic field, and the voltage output was about 55.4175 mV when external DC magnetic field was zero. We define the minimum voltage difference that can clearly distinguish response signal to DC magnetic field and Vout(H_{DC}=0) as the limit resolution. To evaluate the capabilities of AC magnetic field detection for toroidal ME magnetic sensor, the output sensitivity and resolution were measured under a 2.25Oe DC circumferential bias magnetic field. The AC magnetic field sensitivity and resolution were characterized for toroidal ME magnetic sensors using an active method: a toroidal solenoid with 400turn was wound around the toroidal sensor to carry a 90mA DC current provided by a current source. The toroidal ME magnetic field sensor was fixed in the center of the Helmholtz coil, the output terminal of the lock-in amplifier generated a AC voltage of 111.42 kHz for the Helmholtz coil, and the AC magnetic field was controlled, via controlling the output voltage of the phase-locked amplifier. Finally, measure the output signals of the sample at 111.42 kHz by the lock-in amplifier. Fig 5 (b) shown the measurements of low-level magnetic field variations were performed for our toroidal sample at the resonance frequency of f=111.42kHz, and the induced ME voltage exhibits an approximately linear relationship with the AC magnetic field strength and increases with the AC magnetic field over the range of approximately (0.010e-0.110e). The measured sensitivities under a 2.250e circumferential bias magnetic field was about 59.6mV/Oe. The inset of Fig 5 (b) shown the induced ME voltages from the toroidal ME magnetic sensor in response to little changes in an AC magnetic field. The AC magnetic field generated by Helmholtz coil was H_{AC}=7×10⁻⁹T of 111.42kHz. The induced ME voltage output was about 6 µV, the system noise was determined to be about 2 µV, which corresponds to a SNR=9.5dB. And the signal and noise can be clearly distinguished under this low AC magnetic field. Therefore, we define the minimum SNR that can clearly distinguish between signal and system noise as the criteria of limit resolution. The limit of resolution of the toroidal ME magnetic field sensor to AC magnetic field variations of 111.42 kHz is about 7×10^{-9} T.

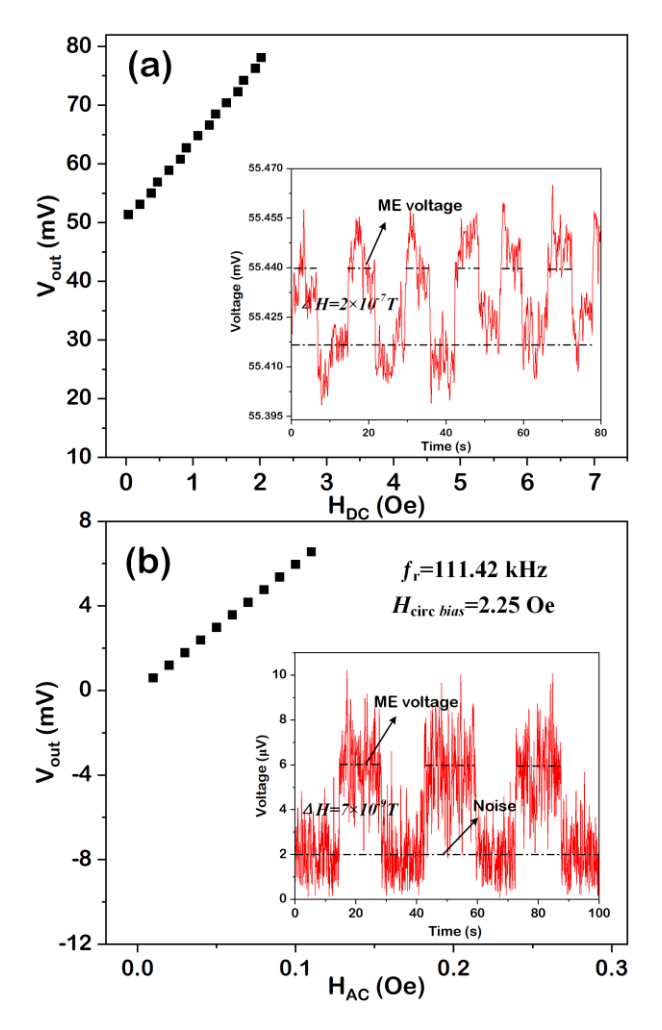


Fig. 5 (a) DC magnetic field sensitivity and resolution measurements implementation under a 111.42 kHz tiny circumferential AC excitation. (b) AC magnetic field sensitivity and resolution measurements implementation under a 2.25 Oe circumferential DC bias magnetic field.

To evaluate the stability of the toroidal magnetic sensor in the detection of planar DC/AC magnetic field, we conducted a one-hour continuous test for DC and AC magnetic field by toroidal magnetic sensor, respectively. The continuous data of the proposed toroidal magnetic sensor when detection a 10e DC magnetic field was recorded, and the results were shown in Fig. 6(a) that all points were within the fluctuation range of 64.55–64.85 mV. And the inset of Fig. 6(a) shown the statistical histogram of 3600 sampling points follows standard normal distribution (mean value μ =64.71667 mV and standard deviation value σ =0.04305 mV). Fig. 6(b) shown the continuous data recorded of the toroidal magnetic sensor when detection a 1.20e AC magnetic field, which all points were within the fluctuation range of 71.4351–71. 5665 mV. And the inset of Fig. 6(b) shown the standard normal distribution of statistical histogram with 3600 points, the mean value μ =71.4511 mV, standard deviation value σ =0.001725 mV. Finally, methodology for evaluating extension uncertainty in statistical analysis were employed to evaluate its stabilities, and the results are detailed in the following:

$$U_{DC}=(64.71667\pm0.147061)$$
mV P=0.99

$$U_{AC}$$
=(71.4511±0.099215)mV P=0.99

Where U denotes the output voltage, P represent the confidence probability. As a result, the uncertainty of the toroidal sensor for DC magnetic and AC magnetic reaches estimated value of 0.147061mV and 0.099215 mV, respectively, which both exhibiting desired stabilities for a long time.

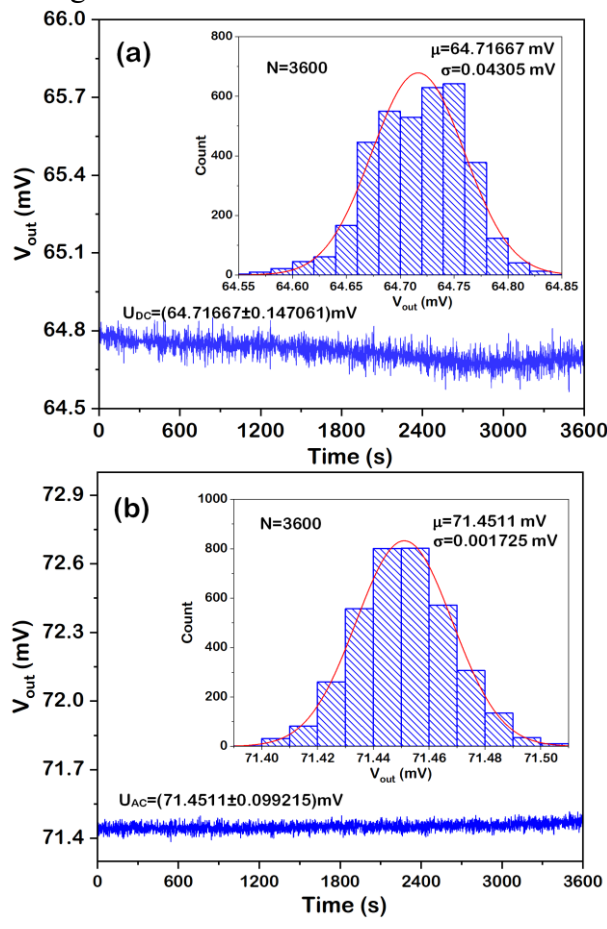


Fig.6 Continuous sampling of output voltage: (a) under constant planar DC magnetic field for 1 h. (b) under resonance and constant planar AC magnetic field for 1 h. The inset shows the histogram for the obtained 3600 sampling points.

IV. CONCLUSIONS

In summary, we have developed a tri-layer toroidal ME magnetic sensor consisting of strictly concentric ferrites/piezoelectric rings with toroidal solenoid around it. Studies on the relationship between the induced ME voltage and the angle of planar AC/DC magnetic field, and its sensitivity, resolution and stability under DC/AC planar magnetic field were systemically characterized. Our toroidal ME magnetic sensor had ultra-low shape-induced anisotropy, the voltage output was almost unaffected by the angle between the ME magnetic sensor and the planar DC/AC magnetic field (see Fig.3). Moreover, under a low excitation of f=111.42 kHz circumferential AC magnetic field, the induced ME voltage of the toroidal ME magnetic sensor to the planar DC magnetic field exhibits an approximately linear relationship over the range of approximately (0.10e-20e), the sensitivities were about 15mV/Oe, and the resolution was about 2×10^{-7} T. Under a 2.250e circumferential DC bias magnetic field, the induced

ME voltage of the toroidal ME magnetic sensor to the planar AC magnetic field of f=111.42kHz exhibits an approximately linear relationship over the range of approximately (0.01Oe-0.11Oe), the sensitivities were about 59.6mV/Oe, and the resolution was about 7×10^{-9} T. The ultra-low shape-induced anisotropy, high sensitivity and high resolution of the toroidal ME magnetic sensor at room temperature provided great potentials for weak magnetic field detection.

ACKNOWLEDGEMENT

This work was financially supported by National Natural Science Foundation of China (NSFC) (Grant Nos. 61973279, 62004177, 62073299), Foundation of Excellent Young Scholars in Henan Province (Grant No. 222300420096), Foundation for University Young Backbone Scholars in Henan Province (Grant No. 2020GGJS122), and Project of Central Plains Science and Technology Innovation Leading Talents (Grant No.224200510026). The research at Russia was supported by the Russian Science Foundation project (Grant No. 22-19-000763). The research at Oakland University was supported by grants from the National Science Foundation (NSF) (Grant Nos. DMR-1808892, ECCS-1923732) and the Air Force Office of Scientific Research (AFOSR) (Award No. FA9550-20-1-0114).

REFERENCES

- [1] Q.Q. Li, L. Chen, M. Li, S.L. Shaw, A. Nuchter, A Sensor-Fusion Drivable-Region and Lane-Detection System for Autonomous Vehicle Navigation in Challenging Road Scenarios, IEEE Trans. Veh. Technol., 63 (2014) 540-555.
- [2] T. Uchiyama, J.J. Ma, Development of pico tesla resolution amorphous wire magneto-impedance sensor for bio-magnetic field measurements, J. Magn. Magn. Mater., 514 (2020) 5.
- [3] Z.Q. Chu, Z.K. Jiang, Z.N. Mao, Y. Shen, J.Q. Gao, S.X. Dong, Low-power eddy current detection with 1-1 type magnetoelectric sensor for pipeline cracks monitoring, Sens. Actuator A-Phys., 318 (2021) 8.
- [4] J. Lenz, A.S. Edelstein, Magnetic sensors and their applications, IEEE Sens. J., 6 (2006) 631-649.
- [5] K.J. Lohmann, C.M.F. Lohmann, L.M. Ehrhart, D.A. Bagley, T. Swing, Animal behaviour Geomagnetic map used in sea-turtle navigation, Nature, 428 (2004) 909-910.
- [6] P.D. Prasad, J. Hemalatha, Enhanced magnetic properties of highly crystalline cobalt ferrite fibers and their application as gas sensors, J. Magn. Magn. Mater., 484 (2019) 225-233.
- [7] Y.M. Mu, P. Li, Y.M. Wen, Mutual inductive magnetic sensor consisting of a pair of coplanar parallel winding spiral coils sandwiched by soft magnetic ribbons, J. Magn. Magn. Mater., 542 (2022) 7.
- [8] L. Rovati, S. Cattini, Zero-Field Readout Electronics for Planar Fluxgate Sensors Without Compensation Coil, IEEE Trans. Ind. Electron., 59 (2012) 571-578.
- [9] U. Ausserlechner, Hall Effect Devices with Three Terminals: Their Magnetic Sensitivity and Offset Cancellation Scheme, J. Sens., 2016 (2016) 16.
- [10] S. Tanaka, Z. Aspanut, H. Kurita, C. Toriyabe, Y. Hatuskade, S. Katsura, Bio-application of high-Tc SQUID magnetic sensor, J. Magn. Magn. Mater., 300 (2006) E315-E319.

- [11] J.T. Zhang, J.H. Liu, Q.F. Zhang, D.A. Filippov, K. Li, J. Wu, J.G. Tao, L.Y. Jiang, L.Z. Cao, G. Srinivasan, High-resolution magnetic sensors in ferrite/piezoelectric heterostructure with giant magnetodielectric effect at zero bias field, Rev. Sci. Instrum., 92 (2021) 7.
- [12] J. Osborne, J. Orton, O. Alem, V. Shah, Fully Integrated, Standalone Zero Field Optically Pumped Magnetometer for Biomagnetism, in: Conference on Steep Dispersion Engineering and Opto-Atomic Precision Metrology XI, Spie-Int Soc Optical Engineering, San Francisco, CA, 2018.
- [13] H. Chiriac, M. Tibu, A.E. Moga, D.D. Herea, Magnetic GMI sensor for detection of biomolecules, J. Magn. Magn. Mater., 293 (2005) 671-676.
- [14] S.X. Dong, J.F. Li, D. Viehland, Ultrahigh magnetic field sensitivity in laminates of TERFENOL-D and Pb(Mg1/3Nb2/3)O-3-PbTiO3 crystals, Appl. Phys. Lett., 83 (2003) 2265-2267.
- [15] S.X. Dong, J.Y. Zhai, J.F. Li, D. Viehland, Small dc magnetic field response of magnetoelectric laminate composites, Appl. Phys. Lett., 88 (2006) 2.
- [16] C.X. Sun, W.R. Yang, Y.F. He, C.Z. Dong, L. Chen, Z.Q. Chu, X.F. Liang, H.H. Chen, N.X. Sun, Low-Frequency Magnetic Field Detection Using Magnetoelectric Sensor With Optimized Metglas Layers by Frequency Modulation, IEEE Sens. J., 22 (2022) 4028-4035.
- [17] S.Y. Yang, J. Xu, X.N. Zhang, S.X. Fan, C.Y. Zhang, Y.C. Huang, Q. Li, X. Wang, D.R. Cao, J. Xu, S.D. Li, Self-biased Metglas/PVDF/Ni magnetoelectric laminate for AC magnetic sensors with a wide frequency range, J. Phys. D-Appl. Phys., 55 (2022) 11.
- [18] J.C. Chen, P. Kan, Z.H. Yu, F. Alrashdan, R. Garcia, A. Singer, C.S.E. Lai, B. Avants, S. Crosby, Z.X. Li, B.S. Wang, M.M. Felicella, A. Robledo, A.V. Peterchev, S.M. Goetz, J.D. Hartgerink, S.A. Sheth, K.Y. Yang, J.T. Robinson, A wireless millimetric magnetoelectric implant for the endovascular stimulation of peripheral nerves, Nat. Biomed. Eng, 6 (2022) 706-716.
- [19] M.J. PourhosseiniAsl, Z.Q. Chu, X.Y. Gao, S.X. Dong, A hexagonal-framed magnetoelectric composite for magnetic vector measurement, Appl. Phys. Lett., 113 (2018) 5.
- [20] J.T. Zhang, K. Li, Q.F. Zhang, D.A. Filippov, J. Wu, J.G. Tao, J. Chen, L.Y. Jiang, L.Z. Cao, G. Srinivasan, Effects of magnetic-elastic anisotropy on magnetoelectric gyrator with ferrite/PZT/ferrite laminate for enhancement of power conversion efficiencies, J. Magn. Magn. Mater., 540 (2021) 9.
- [21] C.S. Zhang, T.Y. Ma, M. Yan, Domain rotation simulation of anisotropic magnetostrictions in giant magnetostrictive materials, J. Appl. Phys., 110 (2011) 6.
- [22] X.X. Cui, S.X. Dong, Theoretical analyses on effective magnetoelectric coupling coefficients in piezoelectric/piezomagnetic laminates, J. Appl. Phys., 109 (2011) 7.
- [23] J.T. Zhang, K. Li, D.Y. Chen, D.A. Filippov, Q.F. Zhang, S.Y. Li, X. Peng, J. Wu, R. Timilsina, L.Z. Cao, G. Srinivasan, Field-Orientation-Dependent Dynamic Strain Induced Anisotropic Magnetoelectric Responses in Bi-layered Ferrite/Piezoelectric Composites (vol, pg,), J. Electron. Mater., 49 (2020) 1577-1577.
- [24] C. Premachandra, D. Ueda, K. Kato, Speed-Up Automatic Quadcopter Position Detection by Sensing Propeller Rotation, IEEE Sens. J., 19 (2019) 2758-2766.
- [25] L.J. Xu, L.Y. Wang, G. Yin, H.W. Zhang, Communication Information Structures and Contents for Enhanced Safety of Highway Vehicle Platoons, IEEE Trans. Veh. Technol., 63 (2014) 4206-4220.
- [26] L.Z. Cao, D.Y. Chen, S.T. Geng, Q.F. Zhang, K. Li, X.X. Hang, B.F. Ge, J.H. Liu, Y. Ruan, R. Timilsina, L.Y. Jiang, J.T. Zhang, Electric-field-controlled frequency tunability enhancement by

- samarium light doping in PZT/Ni-Zn ferrite/PZT magnetoelectric composites, J. Mater. Sci.-Mater. Electron., 30 (2019) 16347-16352.
- [27] J.T. Zhang, D.Y. Chen, K. Li, D.A. Filippov, B.F. Ge, Q.F. Zhang, X.X. Hang, L.Z. Cao, G. Srinivasan, Self-biased magnetoelectric gyrators in composite of samarium substituted nickel zinc ferrites and piezoelectric ceramics, AIP Adv., 9 (2019) 5.
- [28] A. Costa, A.P.A. Diniz, A.G.B. de Melo, R. Kiminami, D.R. Cornejo, A.A. Costa, L. Gama, Ni-Zn-Sm nanopowder ferrites: Morphological aspects and magnetic properties, J. Magn. Magn. Mater., 320 (2008) 742-749.
- [29] J. Ryu, A.V. Carazo, K. Uchino, H.E. Kim, Magnetoelectric Properties in Piezoelectric and Magnetostrictive Laminate Composites, Japanese Journal of Applied Physics, (2001).
- [30] J.T. Zhang, H.W. Zhao, Q.F. Zhang, D.A. Filippov, J. Wu, J.G. Tao, L.Y. Jiang, L.Z. Cao, G. Srinivasan, Disentangling the power transfer process by non-contact optical measurement in nickel-zinc ferrite/piezoelectric magnetoelectric gyrators, J. Magn. Magn. Mater., 524 (2021) 7.
- [31] S.X. Dong, J.R. Cheng, J.F. Li, D. Viehland, Enhanced magnetoelectric effects in laminate composites of Terfenol-D/Pb(Zr,Ti)O-3 under resonant drive, Appl. Phys. Lett., 83 (2003) 4812-4814.
- [32] S.X. Dong, J.F. Li, D. Viehland, A longitudinal-longitudinal mode TERFENOL-D/Pb(Mg1/3Nb2/3)O-3-PbTiO3 laminate composite, Appl. Phys. Lett., 85 (2004) 5305-5306.
- [33] S. Chen, X.F. Yang, J. Ouyang, G.Q. Lin, F. Jin, B. Tong, Fabrication and characterization of shape anisotropy AlN/FeCoSiB magnetoelectric composite films, Ceram. Int., 40 (2014) 3419-3423.
- [34] S.X. Dong, J.F. Li, D. Viehland, J. Cheng, L.E. Cross, A strong magnetoelectric voltage gain effect in magnetostrictive-piezoelectric composite, Appl. Phys. Lett., 85 (2004) 3534-3536.
- [35] J.T. Zhang, B.F. Ge, Q.F. Zhang, D.A. Filippov, J. Wu, J.G. Tao, Z.C. Jia, L.Y. Jiang, L.Z. Cao, G. Srinivasan, Non-reciprocal voltage-current and impedance gyration effects in ferrite/piezoelectric toroidal magnetoelectric composites, Appl. Phys. Lett., 118 (2021) 6.